EFFECT OF SUBSTRATE TEMPERATURE ON STRUCTURAL PROPERTIES OF NANOSTRUCTURED ZINC OXIDE THIN FILMS PREPARED BY REACTIVE DC MAGNETRON SPUTTERING

B.RAJESH KUMAR*, T. SUBBA RAO

Materials Research Lab, Department of Physics, Sri Krishnadevaraya University, Anantapur-515055, A.P, India

In the present work, Zinc oxide (ZnO) thin films have been deposited on glass substrates from room temperature to 673K by using DC magnetron sputtering. Structural properties have been studied by X-ray diffraction (XRD) technique. The preferred orientation for ZnO thin films lies along (0 0 2) direction. From XRD data, the average crystallite size is determined from scherrer formula. The surface morphology and roughness of the films were characterized by Scanning electron microscopy (SEM) and atomic force microscopy (AFM). SEM images shows that grain sizes of Zinc oxide thin films is found to be in the range of 15-28nm.

(Received June 14, 2011; accepted August 30, 2011)

Keywords: ZnO thin film, DC magnetron sputtering, X-ray diffraction, Atomic force microscopy

1. Introduction

Zinc oxide (ZnO) is an n-type II-VI semiconductor with a wide and direct band-gap (E_g =3.3eV at room temperature). It has a wurtzite type crystal structure with a hexagonal symmetry, lattice constants a= 0.325nm, c=0.521 nm and melting point 2248K. The electron Hall mobility at 300K reaches 200 $cm^2V^{-1}S^{-1}$ ($m_e^* = 0.59$) and hole mobility 5-50$cm^2V^{-1}S^{-1}$(m_h^*=0.59). The refractive index of ZnO is in the interval 2.008~2.009[1]. ZnO has a high exciton binding energy (E_B=60meV). Due to the wide E_g and high E_B, ZnO is a promising candidate for optoelectronics devices of short wavelength at room temperature. ZnO films have piezoelectric properties when the crystallites have the c-axis perpendicular to the substrate. As a piezoelectric material it has been used in surface acoustic wave (SAW) filters/resonators, micro actuators and acoustic-optic devices [2-4]. ZnO-based structures have been used for development of UV/blue LEDs [5], laser diodes [6], UV photo detectors (Schottky, MSM) [7, 8], transparent field-effect transistors (TFETs) [9], biomedical sensors, solar cells [10] and saw filters [11].

A number of techniques have been involved for fabrication of ZnO thin films, including chemical vapor deposition, sol-gel, spray-pyrolysis, molecular beam epitaxy, pulsed laser deposition, vacuum arc deposition, and magnetron sputtering [12-18]. Among the methods, magnetron sputtering has several advantages, such as low processing temperature, good adhesion of films on substrates, very good thickness uniformly, high deposition rate and high density of the films with relative ease of scaling to large areas. It is also a simple process, and the process parameters are easy to control. In the present investigation ZnO thin films were deposited by dc magnetron sputtering. The crystalline structures and surface morphology were studied by X-ray diffraction (XRD), Scanning Electron Microscope (SEM) with EDAX and Atomic Force Microscopy (AFM).

Corresponding author *rajphyind@gmail.com*

2. Experimental details

Zinc oxide thin films thin films were prepared by DC reactive magnetron sputtering. High purity metal target of Zinc (99.999%) with 2 inch diameter and 4mm thickness are used for deposition on glass substrates. The base pressure in chamber was $5X10^{-4}$Pa and the distance between target and substrate was set at 60 mm. The glass substrates were ultrasonically cleaned in acetone and ethanol, rinsed in an ultrasonic bath in deionized water for 15 min, with subsequent drying in an oven before deposition. High purity (99.999%) Ar and O_2 gas was introduced into the chamber and was metered by mass flow controllers for a total flow rate fixed at 30sccm. Deposition was carried out at a working pressure of 1Pa after pre-sputtering with argon for 10min. For the Zinc oxide thin films deposition, O_2 flow rate is 2 sccm and the deposition time is 25min. The sputtering power was maintained at 110W during deposition.

The depositions were carried out from room temperature (RT) to 400°C. Film thickness was measured by Talysurf thickness profilometer. The resulting thickness of all the films is about 600nm. XRD patterns of the films were recorded with the help of Philips (PW 1830) X-ray diffractometer using CuKα radiation. The tube was operated at 30 KV, 20mA with the scanning speed of 0.030(2θ)/sec. Surface morphology of the samples has been studied using HITACHI S-3400 Scanning Electron Microscope (SEM) with Energy Dispersive Analysis of X-rays (EDAX). EDAX is carried out for the elemental analysis of prepared samples. The surface roughness of ZnO films were examined by atomic force microscopy (AFM; Veeco Instruments Inc, USA)

3. Results and Discussion

Figure 1(a)-(e) shows the X-ray diffraction(XRD) patterns of ZnO thin films deposited on glass substrate from 303K (room temperature, RT) to 673K.The X-ray diffractions have been performed for diffraction angles between 10 °C to 70 °C . The (0 0 2) diffraction peak at about 34°C could be found for all the films. The films exhibit the preferred c-axis orientation due to the minimal surface energy in the ZnO wurtzite structure. The crystallites are highly oriented with their c-axes perpendicular to the plane of the substrate. The average crystallite size D, was evaluated from the full-width-half-maximum (FWHM) value of the (0 0 2) reflections using the Scherrer equation:

$$D= 0.9\lambda/(\beta \cos\theta) \tag{1}$$

Where β is angular FWHM of the diffraction line in radians, and λ is the X-ray wavelength. The film stress σ, parallel to the film surface was calculated using the relation [19]. The calculated average crystallite size from XRD (D_{XRD}) was found to be in the range of 13-36nm. It is observed that the crystallite size increases with increase of substrate temperature. The increase of the crystallite size and the improvement of the crystallinity are responsible for the decreasing the resistivity due to diminishing in grain boundary scattering. The film stress parallel to the film surface was calculated using the relation [22].

$$\sigma = [2 C^2_{13} - C_{33} (C_{11}+C_{12}) (c-c_o) / (2C_{13}) c_o] = -233[(c-c_o)/c_o] \tag{2}$$

Where C_{ij} coefficients are the elastic stiffness constants of ZnO single crystals: C_{11} = 208.8 GPa, C_{12} = 119.7 GPa, C_{13}= 104.2 GPa, C_{33}= 213.8 GPa, c and c_o are the measured and stress free c-axis lattice constants respectively. The negative sign equation (2) corresponds to compressive stress. The c value calculated from the (0 0 2) reflection peak using Bragg's law and the c_o value was 0.5206nm using the diffraction wavelength [20]. The film stress values shown in table 1 have a tensile stress for 303K, 373K and 473K substrate temperatures, whereas for the thin films deposited at substrate temperatures 573K and 673K has compressive stress.

Table. 1. Effect of substrate temperature on structure parameters of nanostructured ZnO thin films

S.No	Substrate Temperature(K)	Stress (GPa)	D $_{XRD}$ nm
1	303	1.16	13.5
2	373	0.62	18.6
3	473	0.13	21.1
4	573	-0.26	27.4
5	673	-0.53	36.1

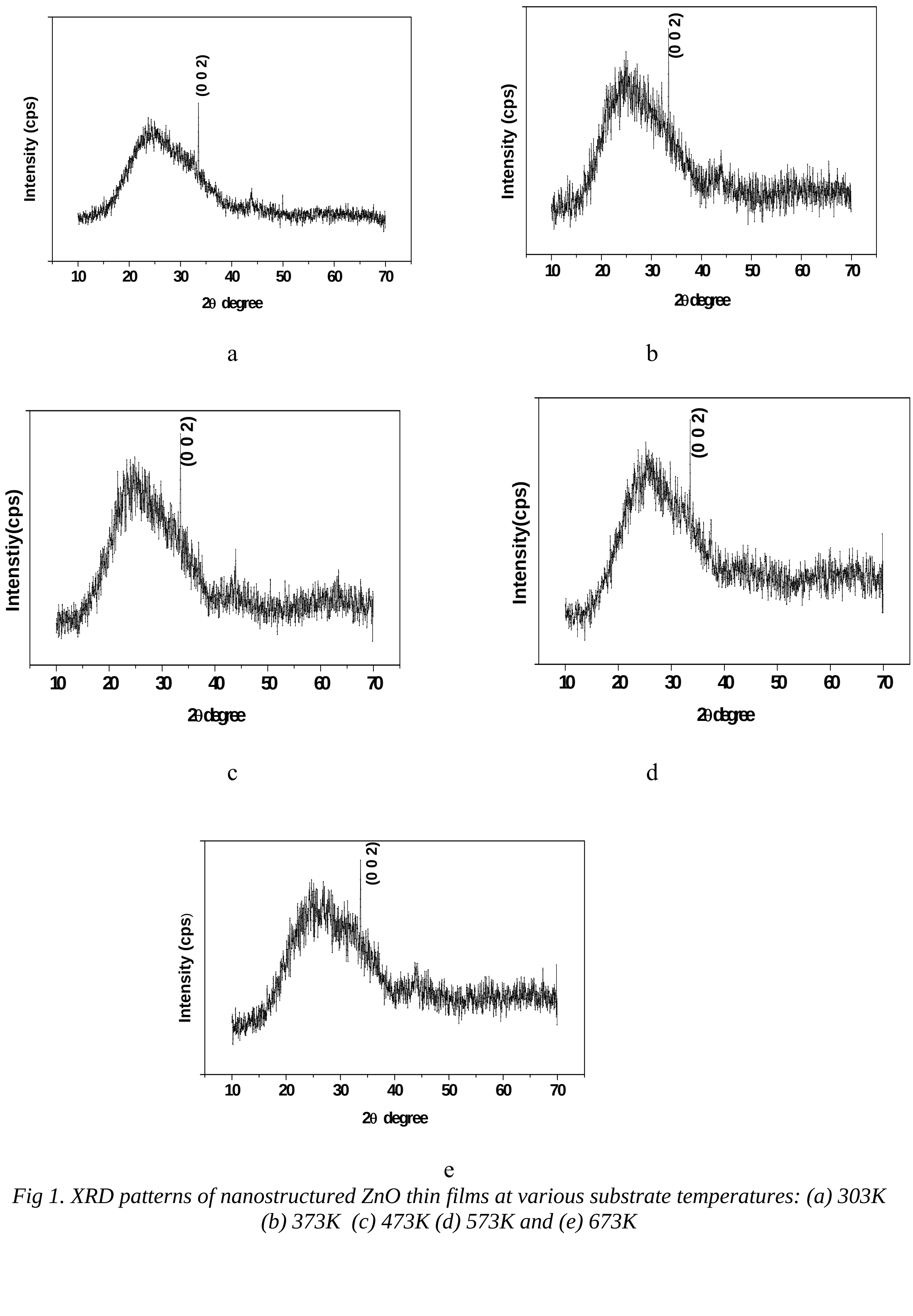

Fig 1. XRD patterns of nanostructured ZnO thin films at various substrate temperatures: (a) 303K (b) 373K (c) 473K (d) 573K and (e) 673K

SEM images of nanostructured ZnO thin films deposited on glass substrate at temperatures 303K, 373K, 473K, 573K and 673K are shown in figure 2(a) – 2(e). Figures 2(a) and 2(b) shows nanoclusters with small grains inside. With increase of substrate temperature SEM images shown in figure 2(c) -2(e) have a regularly shaped grains. The average grain size is found to be 15.3nm, 18.5nm 20.2nm, 23.4nm and 28 nm respectively for 303K, 373K, 473K, 573K and 673K. EDAX plots with their elemental compositional data are shown in figure 3(a) - 3(e). Similar results were obtained by Zhenwei Li et al [21].

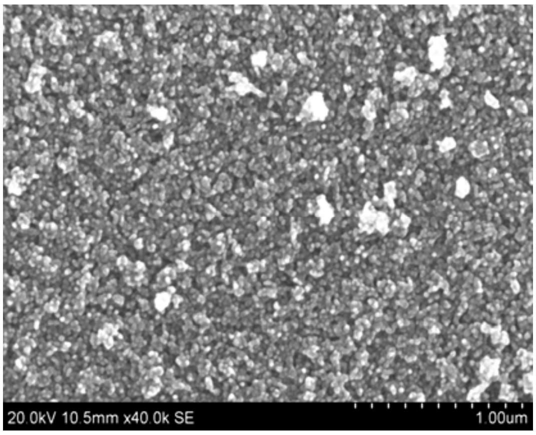

a

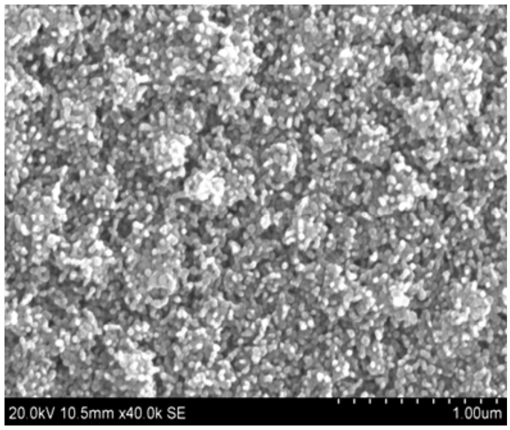

b

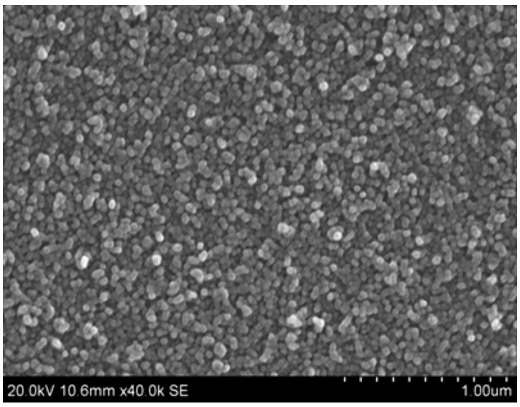

c

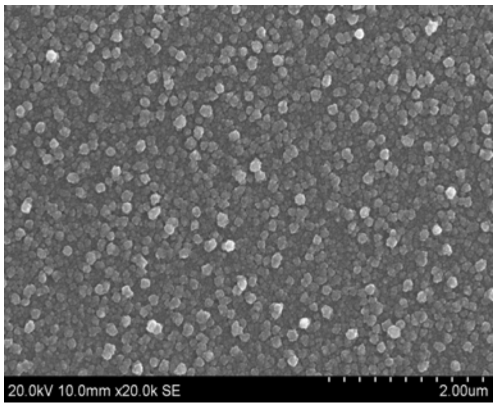

d

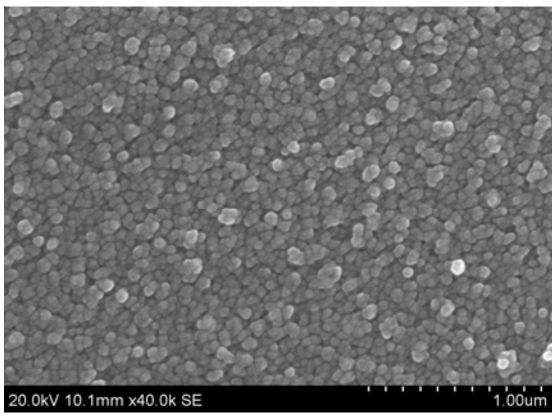

e

Fig 2. SEM images of nanostructured ZnO thin films obtained at substrate temperatures: (a) 303K (b) 373K (c) 473K (d) 573K and (e) 673K

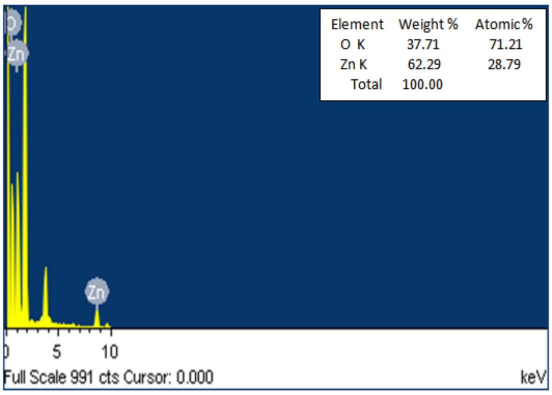

a

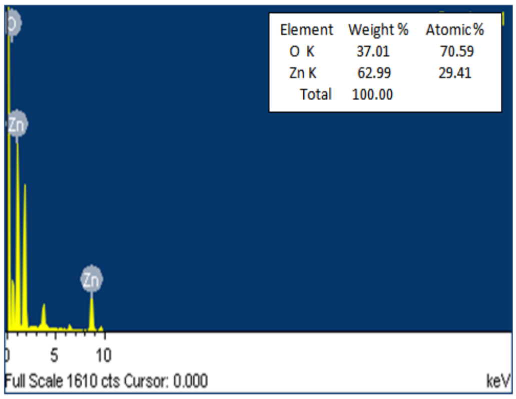

b

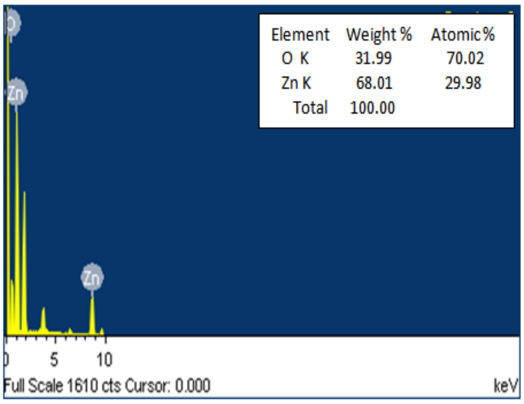

c

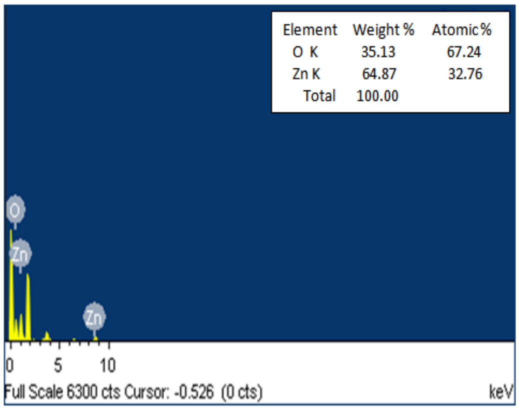

d

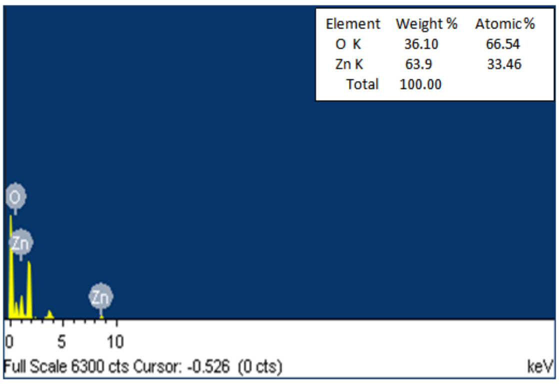

e

Fig 3. EDAX plots of nanostructured ZnO thin films at different substrate temperatures :(a) 303K (b) 373K (c) 473K (d) 573K and (e) 673K

The AFM analysis provides measure of surface roughness and average grain size with data accuracy of ±0.3nm. Figure 4(a)-4(d) shows typical surface AFM images (in three-dimensional and two-dimensional) of ZnO films deposited on glass substrate at 373K, 473K, 573K and 673K substrate temperatures. The surface roughness was measured over 1µ X 1µ regions. The scale at the left corner of each AFM image indicates the range from the lowest point to the highest grain peak. In Table 1the average surface roughness (RMS) values and the average surface grain diameters are listed. The RMS values are found to be 8.07nm, 8.48nm, 9.48 nm and 10.7 nm respectively for thin films deposited at 373K, 473K, 573K and 673K substrate temperatures. The average grain size is in the range 14nm-31nm, increasing with substrate temperature.

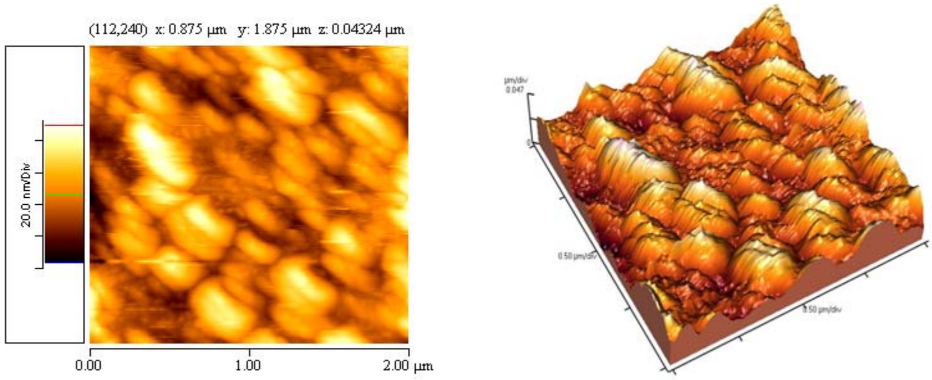

Fig 4 (a)

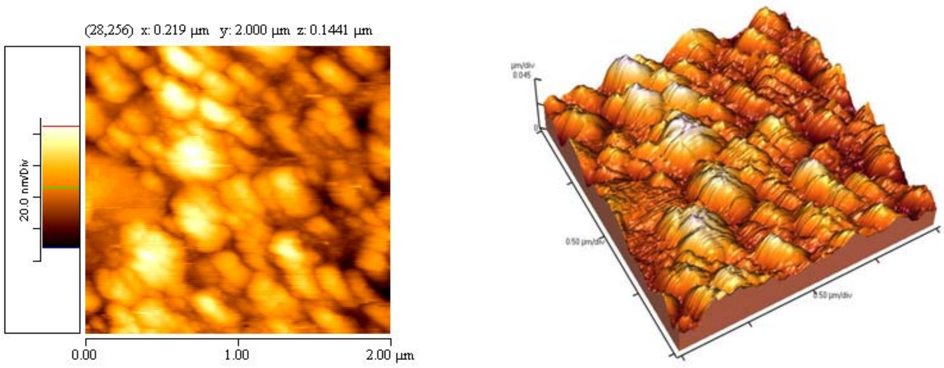

Fig 4 (b)

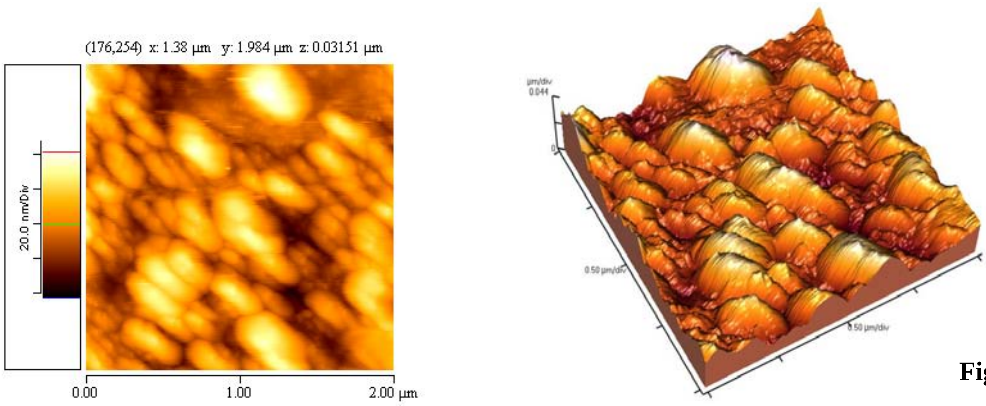

Fig 4 (c)

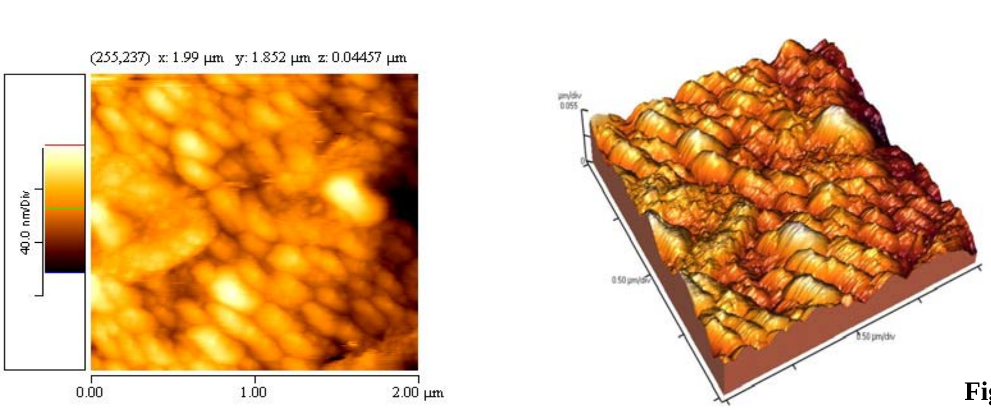

Fig 4 (d)

Fig 4. AFM images of the surface of ZnO thin films deposited at substrate temperatures (a) 373K (b) 473K (c) 573K and (d) 673K

4. Conclusion

ZnO thin films were deposited onto glass substrate with DC reactive magnetron sputtering. All films had a nanostructured feature and showed (0 0 2) plane preferential orientation. SEM images of films deposited at higher substrate temperature shows a clear uniform grains. From AFM, the surface morphology becomes smoother for samples grown at higher substrate temperature that may originate from a decrease in the films's grain size due to the thermal energy provided from more intensive bombardment. The substrate temperatures have a significant influence on the preferential orientation of crystalline structure and formation of nanostructures.

Acknowledgements

The authors are thankful to University Grant Commission (UGC), New Delhi, India for financial support under the project (F.NO.37-346/2009, SR).

References

[1] Daniel Hasko, Jaroslav Bruncko, Vacuum, **84**, 166 (2010).
[2] J.J.Chen, Y.Gao, F.Zeng, D.M.Li, F.Pan, Applied Surface Science, **223**, 318(2004).
[3] J.B.Lee, H.J.Lee, S.H.Seo, J.S.Park, Thin Solid Films, **398**, 641 (2001).
[4] E.S. Kim, R.S.Muller, IEEE Electron.Dev.Lett. **8**, 467 (1987).
[5] J.H.Lim, Ch.K.Kang, K.K.Kim, I.K.Park, D.K.Hwang, S.J.Park, Adv Mater, **18**, 2720(2006).
[6] G. Tobin, E.McGlynn,M.O.Henry, J.P.Mosnier, J.G.Lunney,D. O'Mahony et al, Physica B, **245**,340 (2003).
[7] S.Liang, H.Sheng, Y.Liu, Z.Huo, Y.Lu, H.Shen, J.Cryst Growth, **225**, 110 (2001)
[8] T.K.Lin, S.J.Chang, Y.K.Su, B.R.Huang, M.Fujita, Y.Horikoshi, J. Cryst Growth, **281**, 513(2005).
[9] K.Nomura, H. Ohta, A.Takagi, T.Kamiya, M.Hiranao, H.Hosono, Nature , **432**, 488(2004).
[10] A.E. Suliman, Y.Tang, L.Xu, Sol. Energ. Mat. Sol. C, **91**, 1658(2007).
[11] N.W.Emanetoglu, C.Gorla, Y.Liu, S.Liang, Y. Lu, Mat .Sci. Semicon. Proc., **2**, 247(1999).
[12] B.S.Li, Y.C.Liu, Z.S.chu, D.Z.Shen, Y.M.Lu, J.Y.Zhang, X.W, Fan, J. Appl.Phys., **91**,501(2002).
[13] M.J.Alam, D.C.Cameron, J.Vac. Scie. Technol. **A 19**, 1642 (2001).
[14] A.J.C.Fiddes, K.Durose, A.W. Brinkman, J.Woods, P.D.Coates, A.J.Banister, J.Cryst. Growth, **159**,210(1996).
[15] T.Ohgaki, N.Ohashi, H.Kakemeoto, S.Wada, Y.Adachi, H.Haneda, T.Tsurumi, J.Appl.Phys., **93**, 1961(2003).
[16] Y.R.Ryu, S.Zhu, J.D.Budai, H.R.Chandrasekhar, P.F.Miceli, H.W.White, J.Appl.Phys., **88**, (2000)201.
[17] T.Minami, S.Ida, T.Miyata, Thin Solid Film, **416**, 92(2002).
[18] K.H.Kim, K.C. Park, D.Y.Ma, J.Appl.Phys., **81**,7764 (1997).
[19] Y.G.Wang, S.P.Lau, H.W.Lee, S.F.Yu, B.K.Tay, J.Appl.Phys., **94**, 1597(2003).
[20] T.David, S.Goldsmith, R.L.Boxman, J.Phys. D: Appl.Phys., **38**, 2407(2005).
[21] Zhengwei Li, W. Gao, Materials Letters, **58**, 1363(2004).